

# Minimum detection windows, PI-line existence and uniqueness for helical cone-beam scanning of variable pitch

Yangbo Ye<sup>a)</sup> and Jiehua Zhu

*Department of Mathematics, University of Iowa, Iowa City, Iowa 52242*

Ge Wang

*Department of Radiology, University of Iowa, Iowa City, Iowa 52242*

(Received 19 October 2003; revised 12 December 2003; accepted for publication 16 December 2003; published 18 February 2004)

The goal of this paper is to study Cone-beam CT scanning along a helix of variable pitch. First the rationale and applications in medical imaging of variable pitch CT reconstruction are explained. Then formulas for the minimum detection window are derived. The main part of the paper proves a necessary and sufficient condition for the existence and uniqueness of PI-lines inside this variable pitch helix. These results are necessary steps toward an exact reconstruction algorithm for helix scanning of variable pitch, generalizing Katsevich's formula on constant pitch exact reconstruction. It is shown through an example that, when the derivative of the pitch function is not convex, or when the pitch function passes a inflection point and begins to slow down, PI-lines may be not unique near the rim of the helix cylinder. The conclusion is that the restriction on the pitch function is weaker, if the object is placed well within the helix cylinder and far from its rim, in order to preserve the uniqueness of PI-lines. If the object is near the rim, the restriction condition on the allowable pitch functions becomes stronger. © 2004 American Association of Physicists in Medicine. [DOI: 10.1118/1.1646041]

Key words: Cone-beam CT, helical scanning, CT angiography, minimum detection window, PI-line

## I. INTRODUCTION

Recently, helical CT began a transition from fan-beam to cone-beam geometry with the introduction of multi-slice systems. These narrow-angle cone-beam spiral CT scanners will eventually be refined with wide cone-beam apertures. Helical cone-beam CT uses a two-dimensional 2-D detector array, allowing for a larger scanning range in shorter time with higher image quality, and has important biomedical applications. Contrast-enhanced CT angiography (CTA) attracts increasingly more attention to depict vascular structures. CT fluoroscopy (CTF) provides real-time tomographic images that may be used to initiate spiral CT scanning upon contrast bolus arrival.

The intravascular contrast bolus travels fast in the torso and slowly in the legs. There can be substantial differences in flow velocity between the legs when asymmetric peripheral vascular disease exists. Scanning too early may result in an over-estimation of stenosis, while scanning too late may result in an overlap of venous structures. Various methods were developed to individualize scan timing during constant-speed helical CTA. The fundamental limitation of all these methods is the inability to match the table translation to the bolus propagation. With a pre-set scanning speed, it is difficult and often impossible to synchronize the imaging aperture with the moving bolus peak. Misalignment may be even more problematic when the scanning speed is fast, contrast volume is small and/or the injection rate is high (leading to reduced peak duration) or there are large or small capacity vessels, either from aneurysm formation or occlusive diseases.

To address the above important problem, we propose to drive the patient table and/or the scanner gantry at a variable speed, so that the scanning aperture can be synchronized with the moving bolus peak.<sup>1</sup> Therefore, the image quality can be optimized at the minimum radiation and contrast doses. Our bolus-chasing approach<sup>2</sup> is a significant advancement over the current "bolus-chasing" techniques. The existing techniques use a relatively straightforward estimation of bolus propagation. Our approach utilizes a model based on bolus propagation data, and relies heavily on modern adaptive control techniques. Our project combines real-time imaging, individualized modeling, adaptive and robust control, as well as a state-of-the-art apparatus with high hopes to surpass the limitations of current CTA. As a result, we are naturally led to the mode of helical cone-beam scanning with variable pitch.

In 2003, Katsevich<sup>3,4</sup> established a theoretically exact reconstruction framework in the case of helical cone-beam scanning. The algorithm can be implemented in three steps: (1) 1-D differentiation of cone beam data with respect to the scanning angle, (2) 1-D filtration upon the cone-beam data derivatives, and (3) 3-D backprojection. The work by Katsevich is based on the Tam–Danielsson detection geometry. When cone-beam x-rays come from a point source, the upper and lower half turns of the scanning locus are projected onto a detector plane, which define the boundaries of the so-called Tam–Danielsson detection window. This configuration acquires a minimum amount of data for an exact and robust reconstruction. It is well known that any point inside the

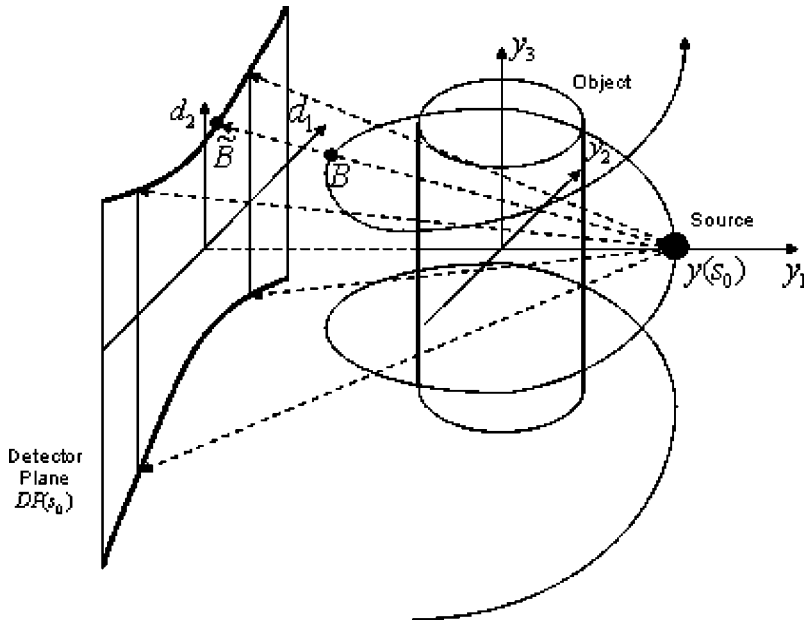


FIG. 1. Minimum detection window delimited by the projected upper and lower turns of the helical locus.

scanning helix is on the one and only so-called PI-line, which is delimited by two points on a helical turn. Quite surprisingly, cone-beam projections collected outside the helical segment associated with the PI-line do not contribute to the reconstruction at that point. This finding significantly improves our understanding of helical cone-beam CT as intended to solve the long object problem.

For the development of our proposed bolus-chasing CTA technology, we propose to generalize Katsevich’s work from the standard-helical scanning geometry to the case of cone-beam helical scanning with a variable pitch. For that purpose, in this paper we study the minimum detection window, PI-line existence and uniqueness in the case of helical cone-beam scanning with variable pitch. In the following, we first describe the extended Tam–Danielsson window, then establish the existence of the PI-line in this case and formulate the conditions under which the PI-line is unique. Also, we give a number of examples to support our analytic results. Finally, we discuss a few of the relevant issues and directions for further research.

**II. MINIMUM DETECTION WINDOW**

Minimum detection windows for standard helices with constant pitch, called Tam–Danielsson windows,<sup>5,6</sup> have been widely used in all exact and nonexact algorithms of the PI-detector. Consider a helix with variable pitch,

$$C(s) = (R \cos(s), R \sin(s), h(s)). \tag{2.1}$$

In this case, we define the minimum detection window at  $s_0$  as the region in the detector plane bounded by the cone beam projections of the upper turn and lower turn of the spiral starting at  $y(s_0)$ .

Figure 1 illustrates the geometry for a minimum detection window. For convenience we assume that the detector plane is parallel to the axis of the helix and is tangent to the spiral cylinder  $y_1^2 + y_2^2 = R^2$ , but in Fig. 1 the detector plane is

drawn slightly away from the cylinder to get a better view. In the detector plane, any object point within the two consecutive turns are projected onto the region between  $\Gamma_{top}$  and  $\Gamma_{bot}$ , the boundaries of the detector plane. Now we deduce the boundary equations of  $\Gamma_{top}$  and  $\Gamma_{bot}$  for the minimum detection window for the x-ray source  $y(s_0)$ .

Let  $B = B(R \cos s, R \sin s, h(s))$  be any point on the next spiral turn above  $y(s_0)$ , and  $\bar{B}$  the cone beam projection of  $B$ . The top and front views of the geometric situation are given in Fig. 2. From the  $y_1 y_2$ -plane,  $\cos \alpha = \sin[(s - s_0)/2]$ , because the triangle BOS is isosceles. Therefore,

$$d_1 = 2R \tan \alpha = \frac{2R \sin(s - s_0)}{1 - \cos(s - s_0)}. \tag{2.2}$$

From the  $y_1 y_3$ -plane,

$$\frac{h(s) - h(s_0)}{d_2} = \frac{R \cos s_0 - R \cos s}{2R \cos s_0 + d_1 \sin s_0};$$

consequently,

$$d_2 = \frac{(h(s) - h(s_0))(2R \cos s_0 + d_1 \sin s_0)}{R(\cos s_0 - \cos s)}$$

$$= \frac{2(h(s) - h(s_0))}{1 - \cos(s - s_0)}. \tag{2.3}$$

Equations in (2.2) and (2.3) are boundary equations for our minimum detection window:

$$d_1 = \frac{2R \sin(s - s_0)}{1 - \cos(s - s_0)}, \quad d_2 = \frac{2(h(s) - h(s_0))}{1 - \cos(s - s_0)},$$

$$\Delta \leq s - s_0 \leq 2\pi - \Delta, \quad \text{or} \quad \Delta - 2\pi \leq s - s_0 \leq -\Delta, \tag{2.4}$$

where  $\Delta = 2 \cos^{-1}(r/R)$  is determined by the ratio of the radii of the object and helix.

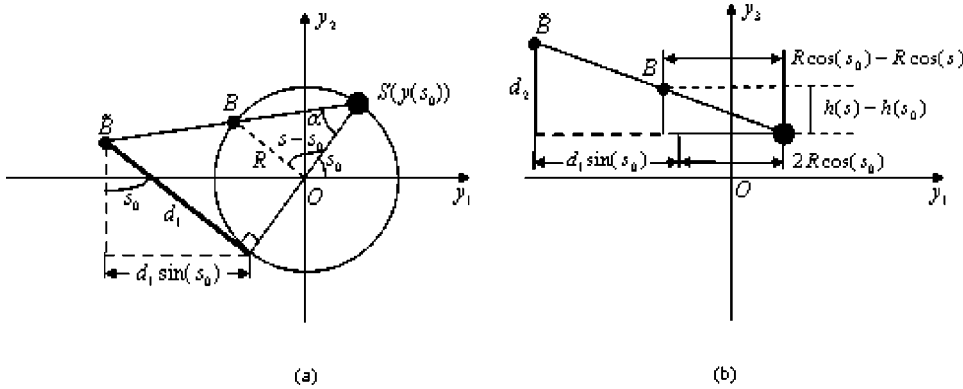


FIG. 2. Views of the projected trajectory of the helical locus. (a) View for the computation of the  $d_1$ ; (b) view for the computation of the  $d_2$ .

Example 2.1: The minimum detection window at  $s=10$  for the helix,

$$C(s) = (2 \cos(s), 2 \sin(s), s^2)$$

and

$$C(s) = (2 \cos(s), 2 \sin(s), s^3)$$

are shown in Fig. 3.

### III. EXISTENCE AND UNIQUENESS CONDITION OF PI-LINE

Let

$$C(s) = (R \cos(s), R \sin(s), h(s)) \tag{3.1}$$

be a helical cone beam scanning path with  $a \leq s \leq b$ ,  $b - a > 4\pi$ . In this equation, the radius of helix  $R$  is a constant, but the pitch is variable. To have the helix going up in the  $z$ -direction as  $s$  increases, we assume that  $h'(s) \geq 0$  for  $s \in [a, b]$  with possible equality held only for finitely many  $s$ .

For any given  $r$  with  $0 < r \leq R$ , consider a region contained completely inside spiral (3.1):

$$U_r = \{(x, y, z) | x^2 + y^2 < r, h(a + 2\pi) \leq z \leq h(b - 2\pi)\}.$$

We will say a point  $P$  is inside the helix, if  $P \in U_r$ . Here we require  $h(a + 2\pi) \leq z \leq h(b - 2\pi)$  in order to guarantee that any point  $P \in U_r$  for  $0 < r \leq R$  is covered by the helix at least one full turn from above and below.

Similar to the case of standard helices with constant pitch,<sup>6</sup> we can define a PI-line of the helix in (3.1) as a line that intersects the helix at two points whose parameters  $s$  are less than 360 degree apart. Given a point  $P$  inside the helix, we want to know if there is one and only one PI-line passing through this point  $P$ .

In this paper, we will give a necessary and sufficient condition on the existence and uniqueness of such a PI-line.

Theorem 3.1—Let  $h(s)$  be a continuous function that is piecewise differentiable. Assume that  $h(s)$  is always increasing with  $h'(s) > 0$  for all  $s \in [a, b]$  but possibly finitely many exceptions. Then for any point  $P = (x_0, y_0, z_0) \in U_r$  there exists a PI-segment passing through  $P$ .

Theorem 3.2—Let  $h(s)$  be a continuous function that is piecewise differentiable. Assume that  $h(s)$  is always increasing with  $h'(s) > 0$  for all  $s \in [a, b]$  but possibly finitely many exceptions. Passing through any point,  $P = (x_0, y_0, z_0) \in U_r$ , there is a unique PI-segment, if and only if

$$(h(s_1) - h(s_2)) \cot \frac{s_2 - s_1}{2} + h'(s_2) + h'(s_1) > 0, \tag{3.2}$$

for any  $s_1$  and  $s_2$  with  $a < s_1 < s_2 < b$  and

$$2 \cos^{-1}(r/R) \leq s_2 - s_1 < \pi, \tag{3.3}$$

with possibly finitely many exceptional  $s_1$  and  $s_2$ .

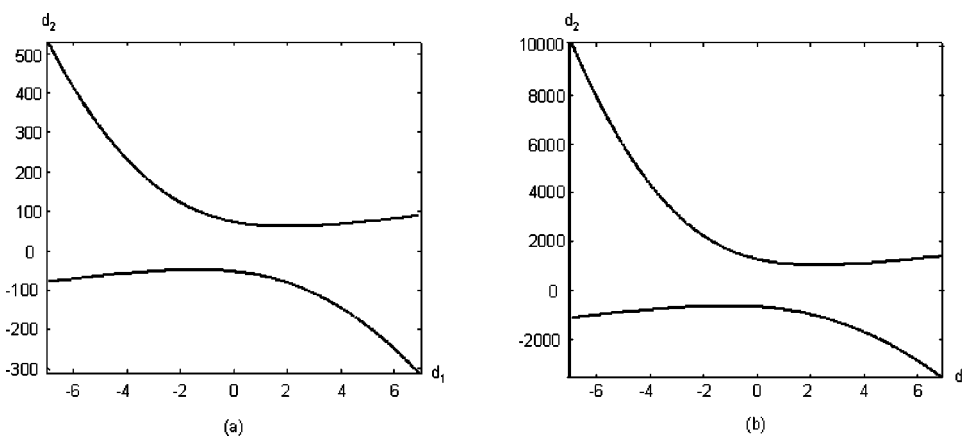


FIG. 3. Minimum detection windows for the generalized helix given in Example 6.1. (a)  $C(s) = (2 \cos(s), 2 \sin(s), s^2)$ ,  $s_0 = 10$ ; (b)  $C(s) = (2 \cos(s), 2 \sin(s), s^3)$ ,  $s_0 = 10$ .

We remark that in (3.2),  $h'(s_1)$  and  $h'(s_2)$  are always positive, while  $h(s_1) - h(s_2)$  is always negative, because  $h(s)$  is assumed to be increasing. Therefore (3.2) is automatically true if  $\pi \leq s_2 - s_1 < 2\pi$ . If the ratio  $r/R$  is small, then  $2 \cos^{-1}(r/R)$  is close to  $\pi$ . Therefore the condition in Theorem 3.2 is less restrictive if  $r$  is smaller, i.e., if the region  $U_r$  is slimmer. The exceptional cases in Theorem 3.1 may consist of points where no derivative exists or  $h'(s) = 0$ .

We may simplify condition (3.2) if we only want to have sufficient conditions.

*Corollary 3.3: Assume that  $h(s)$  is always increasing with  $h'(s) > 0$  for all  $s \in [a, b]$  but possibly finitely many exceptions. Passing through any point  $P = (x, y, z) \in U_r$  there is one and only one PI-line if*

$$(h(s_1) - h(s_2)) \frac{r}{\sqrt{R^2 - r^2}} + h'(s_2) + h'(s_1) > 0, \quad (3.4)$$

for any  $s_1$  and  $s_2$  with  $a < s_1 < s_2 < b$ , with finitely many exceptional  $s_1$  and  $s_2$ .

This corollary can be deduced from Theorem 3.2 by taking  $s_2 - s_1 = 2 \cos^{-1}(r/R)$  so that  $\cot((s_2 - s_1)/2) = r/\sqrt{R^2 - r^2}$ .

*Corollary 3.4: Assume that  $h(s)$  is always increasing with  $h'(s) > 0$  for all  $s \in [a, b]$  but possibly finitely many exceptions. Passing through any point  $P = (x, y, z) \in U_r$  there is one and only one PI-line if  $h'(s)$  is a convex function.*

*Corollary 3.5: Assume that  $h(s)$  is always increasing with  $h'(s) > 0$  for all  $s \in [a, b]$  but possibly finitely many exceptions. Passing through any point  $P = (x, y, z) \in U_r$  there is one and only one PI-line if  $h'''(s) \geq 0$ .*

These two corollaries will be proved in Sec. V.

#### IV. PROOF OF THEOREMS

First we demonstrate the existence of the PI-line geometrically for the helix in (2.1), for a point  $P$  within the helix, as shown in Fig. 4. Let  $L$  be the line parallel to the  $y_3$ -axis passing through point  $P$ . Pick a point  $A$  on the helix, but within the pitch extend  $AP$ . Three cases may occur.

- (1) Case 1. Line  $AP$  intersects the helix at another point  $B$ . Then  $AB$  is a PI-line passing through  $P$ .
- (2) Case 2. Line  $AP$  intersects the helix surface at point  $B$  above the helix.
- (3) Case 3. Line  $AP$  intersects the helix surface at point  $B$  below the helix.

In Case 2 as shown in Fig. 4,  $B'$  is the point on the helix vertically below  $B$ . The line  $AB'$  intersects  $L$  at point  $P'$ ; then  $AB'$  is a PI-line passing  $P'$ . Now rotate the line  $AB'$ , while the line keeps contact with the helix sliding upwards and  $L$ . The line  $A''B''$  is an example which intersects  $L$  at point  $P''$ , above the original point  $P$ . Since this is a continuous process, there is a status of the rotation which contains  $P$ . That line is the PI-line passing  $P$ .

For Case 3, similar geometry arguments can be made by rotating the line  $AB'$  to the helix sliding in the downward direction. These give the existence of the PI-line for the helix (3.1).

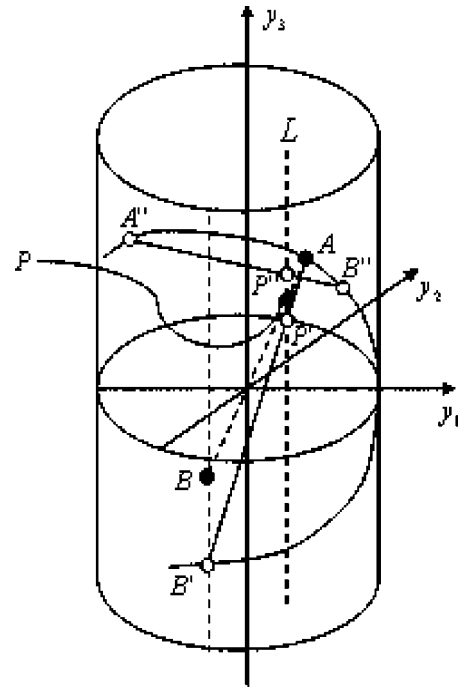


Fig. 4. Geometric argument for the existence of a PI-line for variable pitch helical cone-beam scanning.

Analytically, we can prove the existence and uniqueness of PI-segments in the following way. For any point  $P(x_0, y_0, z_0) = (r_0 \cos \mu_0, r_0 \sin \mu_0, z_0) \in U_r$ , we want to see under what assumption on the function  $h(s)$  the PI-line through  $P$  exists and is unique. A PI-segment from  $(R \cos s_1, R \sin s_1, h(s_1))$  to  $(R \cos s_2, R \sin s_2, h(s_2))$  with  $0 < s_2 - s_1 < 2\pi$  is given by

$$x = Rt \cos s_1 + R(1-t) \cos s_2, \quad (4.1)$$

$$y = Rt \sin s_1 + R(1-t) \sin s_2, \quad (4.2)$$

and

$$z = th(s_1) + (1-t)h(s_2), \quad (4.3)$$

with  $t \in [0, 1]$ . We want to find a unique PI-segment that passes through a given point  $P$ . In other words, we seek a unique triplet  $s_1, s_2, t$  with  $t \in (0, 1)$  and  $0 < s_2 - s_1 < 2\pi$  such that

$$x_0 = Rt \cos s_1 + R(1-t) \cos s_2, \quad (4.4)$$

$$y_0 = Rt \sin s_1 + R(1-t) \sin s_2, \quad (4.5)$$

and

$$z_0 = th(s_1) + (1-t)h(s_2). \quad (4.6)$$

Rewrite (4.4) and (4.5) as

$$r_0 \cos \mu_0 = Rt \cos s_1 + R(1-t) \cos s_2 \quad (4.7)$$

and

$$r_0 \sin \mu_0 = Rt \sin s_1 + R(1-t) \sin s_2, \quad (4.8)$$

for  $0 < s_2 - s_1 < 2\pi$ . Solving these for  $t$  and  $s_2$ , we get

$$t = t(x_0, y_0, s_1) = \frac{R^2 - r_0^2}{2R[R - r_0 \cos(\mu_0 - s_1)]},$$

while  $s_2 = s_2(x_0, y_0, s_1)$  is determined by

$$\cos \frac{s_2 - s_1}{2} = \frac{r_0 \sin(\mu_0 - s_1)}{\sqrt{R^2 + r_0^2 - 2Rr_0 \cos(\mu_0 - s_1)}}.$$

The PI-segment (4.1)–(4.3) contains  $P$  if and only if

$$z = t(x_0, y_0, s_1)h(s_1) + (1 - t(x_0, y_0, s_1))h(s_2(x_0, y_0, s_1)), \tag{4.9}$$

as a function of  $s_1$ , can equal  $z_0$ .

Take  $s_1 = a$ . Since  $0 < s_2 - s_1 < 2\pi$ , we know that  $h(a) < h(s_2) < h(a + 2\pi)$ . Recall that  $0 < t < 1$ . Therefore for  $s_1 = a$ , the right side of (4.9) is less than  $h(s_2)$ , which in turn is less than  $h(a + 2\pi)$ . Similarly, we can show that for  $s_1 = b - 2\pi$ , the right side of (4.9) is greater than  $h(b - 2\pi)$ . Since the right side of (4.9) as a function of  $s_1$  is continuous, there is a solution for any  $z_0$  in the range  $h(a + 2\pi) \leq z_0 \leq h(b - 2\pi)$ . This proves the existence of a PI-segment in Theorem 3.1.

To prove the uniqueness in Theorem 3.2, let us consider the derivative of the function in (4.9):

$$\frac{dz}{ds_1} = (h(s_1) - h(s_2)) \frac{dt}{ds_1} + (1 - t)h'(s_2) \frac{ds_2}{ds_1} + th'(s_1).$$

Differentiating (4.7) and (4.8), we get

$$\frac{dt}{ds_1} = t \cot \frac{s_2 - s_1}{2} \quad \text{and} \quad \frac{ds_2}{ds_1} = \frac{t}{1 - t}.$$

Therefore

$$\frac{dz}{ds_1} = t \left( (h(s_1) - h(s_2)) \cot \frac{s_2 - s_1}{2} + h'(s_2) + h'(s_1) \right).$$

Using this derivative, we know that

$z_0 = t(x_0, y_0, s_1)h(s_1) + (1 - t(x_0, y_0, s_1))h(s_2(x_0, y_0, s_1))$  has a unique solution in  $s_1$  for any  $z_0$  if and only if

$$(h(s_1) - h(s_2)) \cot \frac{s_2 - s_1}{2} + h'(s_2) + h'(s_1) \tag{4.10}$$

is always positive with possibly finitely many exceptions.

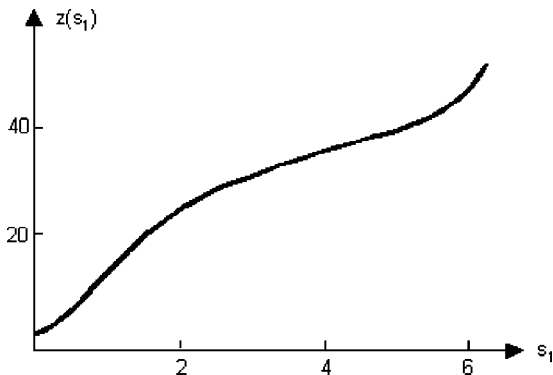


FIG. 5. Function (4.9) for helix (6.2) and  $P(1,0,z_0)$ .

When  $\pi \leq s_2 - s_1 < 2\pi$ , we have  $\cot((s_2 - s_1)/2) < 0$ ,  $h(s_1) - h(s_2) < 0$ ,  $h'(s_1) > 0$ , and  $h'(s_2) > 0$ . Therefore  $dz/ds_1$  is positive for  $\pi \leq s_2 - s_1 < 2\pi$ .

To consider the case of  $0 < s_2 - s_1 < \pi$ , we first point out that (4.7) and (4.8) have solutions in  $t$  for any  $r_0 \leq r$  if and only if  $s_2 - s_1 \geq 2 \cos^{-1}(r/R)$ . This can be seen using a geometric argument. Or, from (4.7) and (4.8) with  $r_0 = r$ , we get

$$\frac{r^2}{R^2} = (t \cos s_1 + (1 - t) \cos s_2)^2 + (t \sin s_1 + (1 - t) \sin s_2)^2. \tag{4.11}$$

The minimum of the right side is attained at  $t = 1/2$ , and at  $t = 1/2$ , (4.11) is reduced to

$$\frac{r^2}{R^2} = \cos^2 \frac{s_2 - s_1}{2}, \quad \text{or} \quad \frac{r}{R} = \cos \frac{s_2 - s_1}{2}.$$

If  $s_2 - s_1 < 2 \cos^{-1}(r/R)$ , this cannot hold.

Therefore, the necessary and sufficient condition on the existence and uniqueness of a PI-segment (4.1)–(4.3) for any point  $P = (x_0, y_0, z_0) \in U_r$  becomes that (4.10) is positive for all  $s_1$  and  $s_2$  in the range  $2 \cos^{-1}(r/R) \leq s_2 - s_1 < \pi$ , with possibly finitely many exceptional  $s_1$  and  $s_2$ . This completes our proof of Theorem 3.2.

### V. PROOF OF COROLLARIES

In this section we assume that  $h'(s)$  is a convex function for  $s \in [a, b]$ . Then (4.10) can be written as

$$\begin{aligned} & (h(s_1) - h(s_2)) \cot \frac{s_2 - s_1}{2} + h'(s_2) + h'(s_1) \\ &= 2 \left( 1 - \frac{s_2 - s_1}{2} \cot \frac{s_2 - s_1}{2} \right) \frac{h(s_2) - h(s_1)}{s_2 - s_1} \\ & \quad + h'(s_2) + h'(s_1) - 2 \frac{h(s_2) - h(s_1)}{s_2 - s_1}. \end{aligned} \tag{5.1}$$

Note that

$$1 - \frac{s_2 - s_1}{2} \cot \frac{s_2 - s_1}{2} > 0,$$

when  $0 < s_2 - s_1 < \pi$ . Using the fact that  $h(s)$  is increasing, we get

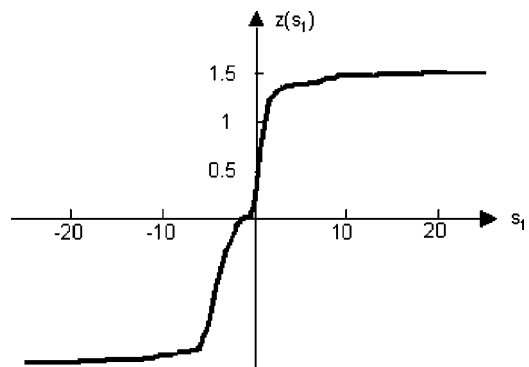


FIG. 6. Function in (4.9) for helix (6.3) and  $P(1,0,z_0)$ .

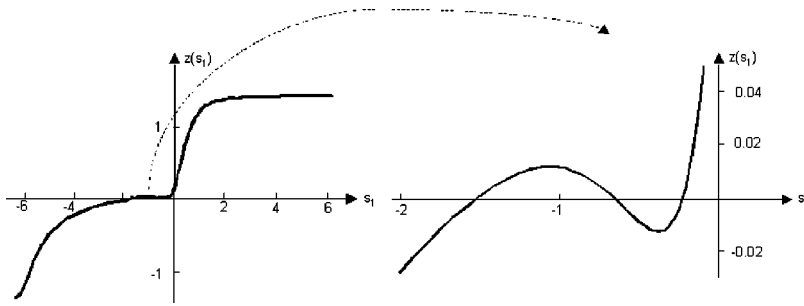


FIG. 7. Function in (4.9) for helix (6.3) and  $P(1.6,0,z_0)$ .

$$2t \left( 1 - \frac{s_2 - s_1}{2} \cot \frac{s_2 - s_1}{2} \right) \frac{h(s_2) - h(s_1)}{s_2 - s_1} > 0. \tag{5.2}$$

The other terms on the right side of (5.1) are equal to

$$\frac{2}{s_2 - s_1} \left[ \frac{1}{2} (h'(s_2) + h'(s_1))(s_2 - s_1) - \int_{s_1}^{s_2} h'(s) ds \right].$$

In the square brackets, the first term is the area of a trapezoid from  $s_1$  to  $s_2$ , while the integral equals the area under the curve of  $h'(s)$  from  $s_1$  to  $s_2$ . The former is larger than the latter, because  $h'(s)$  is a convex. Together with (5.2), we showed that (4.10) is positive in this case, and hence Corollary 3.4 is true.

When  $h(s)$  has the third derivative,  $h'''(s) \geq 0$  implies that  $h'(s)$  is convex. Corollary 3.5 then follows.

**VI. EXAMPLES**

*Example 6.1:* Consider the helix

$$C(s) = (R \cos(s), R \sin(s), s^m), \tag{6.1}$$

for some  $m \geq 2$ . There is one and only one PI-line passing through  $P = (x, y, z) \in U_r$ . In fact, for  $h(s) = s^{2n}$  being an even power, we only consider the helix with  $0 \leq a \leq s \leq b$  due to the assumption  $h'(s) = 2ns^{2n-1} \geq 0$  for  $s \in [a, b]$ . Then

$$h'''(s) = 2n(2n-1)(2n-2)s^{2n-3} \geq 0,$$

for  $n \geq 1$ , and we can apply Corollary 3.5. For instance, when  $h(s) = s^2$ ,

$$\frac{dz}{ds_1} = 2t(s_1 + s_2) \left( 1 - \frac{s_2 - s_1}{2} \cot \frac{s_2 - s_1}{2} \right) > 0.$$

By the proof of Theorem 3.2, we obtain the existence and uniqueness of a PI-line passing through  $P = (x, y, z) \in U_r$ . As a numerical example, function  $z$  defined in (4.9) for the helix,

$$C(s) = (2 \cos(s), 2 \sin(s), s^2), \tag{6.2}$$

and  $P = (1, 0, z_0)$  is shown in Fig. 5; we can see that for  $z_0$  greater than a certain value, there is unique solution satisfying  $z = z_0$ , that is, there is a unique PI-line passing through  $P$ .

For  $h(s) = s^{2n+1}$  being an odd power with some  $n \geq 1$ , we have

$$h'''(s) = (2n+1)2n(2n-1)s^{2n-2} > 0,$$

except  $s = 0$ . Corollary 3.5 thus still applies.

*Example 4.2:* Consider the helix

$$C(s) = (2 \cos(s), 2 \sin(s), \arctan(s)), \tag{6.3}$$

and a point  $P(r, 0, z_0)$  within the helix. For  $r = 1$  and  $r = 1.6$ , the function  $z$  defined in (4.9) for helix (6.3) and point  $P(r, 0, z_0)$  are shown in Fig. 6 and Fig. 7, respectively. It can be seen from the zoom out graph in Fig. 7 that for point  $P(1.6, 0, z_0)$ , when  $z_0$  is within a small neighbor of zero, there are three values of  $s_1$  such that  $z(s_1) = z_0$ , which implies that more than one PI-line passes through  $P(1.6, 0, z_0)$ . But for point  $P = (1, 0, z_0)$ , the uniqueness of PI-lines is true even near zero. These different patterns for different values of  $r$  are due to the property of function  $h(s) = \arctan(s)$ . We have  $h'(s) = 1/(1+s^2)$ . As shown in Fig. 8,  $h(s)$  has an inflection point at  $s = 0$ , and  $h'(s)$  is not convex there. This example explains that for small  $r$ , the condition on the uniqueness of PI-lines is less restrictive, but for larger  $r$  close to  $R$ , the condition on the uniqueness of the PI-line in Theorem 3.2 becomes stronger.

**VII. DISCUSSION AND CONCLUSION**

Based on our studies on the minimum detection window, the PI-line existence and uniqueness with variable pitch helical cone-beam scanning, it seems promising that a

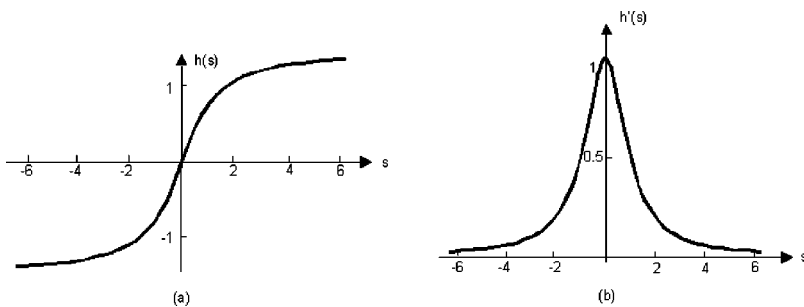


FIG. 8. Change of the concavity of  $h(s)$  at  $s = 0$ . (a) Function  $h(s)$ ; (b) its first derivative as in Example 6.2.

Katsevich-type formula may be established in this case. Similar to what Katsevich did in his proof,<sup>3,4</sup> we may try to use the following steps to prove the exactness of an extended Katsevich formula. First, we express the inner integral in terms of the Fourier transform of the function to be reconstructed,

$$\begin{aligned} & \int_0^{2\pi} \frac{\partial}{\partial q} D_f(y(q), \Theta(s, x, \gamma)) \Big|_{q=s} \frac{d\gamma}{\sin \gamma} \\ &= -\frac{|x-y(s)|}{4\pi} \int_{R^3} \tilde{f}(\xi) (\xi \cdot y(s)) e^{-i\xi \cdot y(s)} \\ & \quad \times \delta(\xi \cdot (x-y(s))) \operatorname{sgn}(\xi \cdot e(s, x)) d\xi, \end{aligned}$$

and show that the reconstruction formula is equivalent to the inverse Fourier transform of that function. This is equivalent to proving that

$$f(x) = \frac{1}{(2\pi)^3} \int_{R^3} \tilde{f}(\xi) B(x, \xi) d\xi$$

is the inverse Fourier transform. Then, the issue becomes to prove if

$$B(x, \xi) \equiv \sum_{s_j \in I_{pf}(x)} \operatorname{sgn}(\xi \cdot y(s_j)) \operatorname{sgn}(\xi \cdot e(s_j, x)) = 1,$$

where multiple 3-D vectors associated with the scanning locus and the detection geometry are involved. By projecting the complicated 3-D relationships into 2-D counterparts, we still have

$$\begin{aligned} & \operatorname{sgn}(\xi \cdot y(s_j)) \operatorname{sgn}(\xi \cdot e(s_j, x)) \\ &= \operatorname{sgn}(\hat{\xi} \cdot y(s_j)) \operatorname{sgn}(\hat{\xi} \cdot \hat{e}(s_j, x)). \end{aligned}$$

Finally, we may prove the correctness of the extended Katsevich formula by exclusively evaluating all the possible geometric configurations of the vectors. If that scheme does not work, we will perform explicit constructions according to

either Tuy's formulation<sup>7</sup> or Grangeat's formula.<sup>3,4,8</sup> The results along these directions will be reported later.

In conclusion, we have established a theoretical foundation for an exact reconstruction of a spiral cone-beam CT scheme with a variable pitch helix.

## ACKNOWLEDGMENTS

This work is partially supported by a Carver Scientific Research Initiative Grant and an NIH/NIBIB grant (EB002667). The authors would like to express their thanks to Dr. Wenxiang Cong and Mr. John Meinel of the CT/Micro-CT Lab, the University of Iowa, for helpful discussions, and to the referees for detailed informative comments.

<sup>a)</sup>Electronic mail: yangbo-ye@uiowa.edu

<sup>1</sup>G. Wang, G. M. Raymond, Y. Li, G. D. Schweiger, M. J. Sharafuddin, A. H. Stolpen, S. Yang, Z. Li, J. B. Bassingthwaite, and M. W. Vannier, "Model of intravenous bolus propagation for optimization of contrast enhancement," *Proc. SPIE* **3978**, 436–447 (2000).

<sup>2</sup>G. Wang and M. W. Vannier, "Bolus-chasing angiography with adaptive real-time computed tomography," U.S. Patent 6,535,821, allowed on 11/26/2002, issued on 3/18/2003.

<sup>3</sup>A. Katsevich, "A general scheme for constructing inversion algorithms for cone beam CT," *Int. J. Math. Math. Sci.* **21**, 1305–1321 (2003).

<sup>4</sup>A. Katsevich, "Improved exact FBP Algorithm for spiral CT," preprint, 2003.

<sup>5</sup>K. C. Tam, "Three-dimensional computerized tomography scanning method and system for large objects with small area detector," U.S. Patent 5,390,112, 1995.

<sup>6</sup>P. E. Danielsson, P. Edholm, J. Eriksson, and S. M. Magnusson, "Towards exact reconstruction for helical cone-beam scanning of long object. A new detector arrangement and a new completeness condition," *Proceedings of the 1997 Meeting on Fully 3D Image Reconstruction in Radiology and Nuclear Medicine*, Pittsburgh, PA, edited by D. W. Townsend and P. E. Kinahan, pp. 141–144.

<sup>7</sup>G. H. Chen, "An alternative derivation of Katsevich's cone-beam reconstruction formula," *Med. Phys.* **30**, 3217–3226 (2003).

<sup>8</sup>M. Defrise, F. Noo, and H. Kudo, "A solution to the long-object problem in helical cone-beam tomography," *Phys. Med. Biol.* **45**, 623–643 (2003).